0026-895X/95/050825-10$3.00/0

MOLECULAR PHARMACOLOGY, 48:825–834 (1995).

Role of Oxidative Stress Generated from the Mitochondrial Electron Transport Chain and Mitochondrial Glutathione Status in Loss of Mitochondrial Function and Activation of Transcription Factor Nuclear Factor-κB: Studies with Isolated Mitochondria and Rat Hepatocytes

CARMEN GARCÍA-RUIZ, ANNA COLELL, ALBERT MORALES, NEIL KAPLOWITZ, and JOSÉ C. FERNÁNDEZ-CHECA

Liver Unit, Department of Medicine and Servicio de Bioquímica, Hospital Clinic i Provincial, and Instituto de Investigaciones Biomédicas August Pi i Suñer, CSIC-Universidad de Barcelona, Barcelona, 08036 Spain (C.G.-R., A.C., A.M., J.C.F.-C.), and Division of Gastrointestinal and Liver Diseases, University of Southern California School of Medicine, Los Angeles, California 90033 (N.K.)

Received April 20, 1995; Accepted August 16, 1995

SUMMARY

Mitochondria are an important source of reactive oxygen intermediates because they are the major consumers of molecular oxygen in cells. Respiration is associated with toxicity, which is related to the activation of oxygen to reactive intermediates. The purpose of the present study was to examine the role of reduced glutathione (GSH) in the maintenance of mitochondrial functions during oxidative stress induced through selective inhibition of the complex III segment of the electron transport chain. Hydrogen peroxide monitored by the fluorescence of dichlorofluorescein increased in a time- and dose-dependent manner on incubation of mitochondria with antimycin A (AA), an inhibitor of complex III. However, blockade of complex I or II with rotenone or thenoyltrifluoroacetone, respectively, did not result in accumulation of hydrogen peroxide. Depletion of mitochondrial GSH to 10–20% of control by preincubation with diethylmaleate (0.8 mM) or ethacrynic acid (250 μM) also increased dichlorofluorescein and malondialdehyde levels and resulted in an additional (2–3-fold) increase after AA. Similar results were obtained when mitochondrial GSH depletion was produced by treatment with buthionine L-sulfoximine before mirochondria isolation. The endogenous oxidative stress induced by AA was accompanied by a moderate loss of activity of ATPase complex (77% of control) and complex IV of respiration (75% of control), which was accentuated after depletion of mitochondrial GSH (51% and 45% of control, respectively). Similar results were observed in isolated hepatocytes in which depletion of mitochondrial GSH and AA led to peroxidation and mitochondrial dysfunction. In addition, with electrophoretic mobility shift assay of the transcription factor nuclear factor-κB (NF-κB), we detected its activation in response to AA (2–3-fold). Depletion of mitochondrial GSH in hepatocytes (20% of control) led to further enhancement of NF-κB activation (2–4-fold), which correlated with generation of hydrogen peroxide. Thus, our results suggest that GSH protects mitochondria against the endogenous oxidative stress produced at the ubiquinone site of the electron transport chain. Mitochondrial GSH depletion potentiates oxidant-induced loss of mitochondrial functions. Oxidant stress in mitochondria can promote extramitochondrial activation of NF-κB and therefore may affect nuclear gene expression.

Oxidants are produced at a high rate as a byproduct of aerobic metabolism. These oxidants include superoxide, hydrogen peroxide, hydroxyl radical, and, possibly, singlet oxygen. They can damage cellular macromolecules, including DNA, protein, and lipids (1–4). Mitochondria constitute the greatest source of ROS as the mitochondrial electron transport system consumes ~85–90% of the oxygen utilized by the cell (3). Intrinsic to this process is the generation of ROS derived from specific segments of the electron transport chain, mainly at the ubiquinone site of the complex III of respiration, which activates molecular oxygen to superoxide anion and, in turn, can lead to formation of other potent oxygen-derived free radicals (5).

In eukaryotes, regulation of gene transcription can be dramatically enhanced by the binding of sequence-specific DNA

This work was supported by Grant AA09526 from the National Institute of Alcohol Abuse and Alcoholism (N.K., J.C.F.-C.), Grant PB92–1110 from Dirección General Política Científica y Técnica, Grant 94–0046/01 from Fondo Investigaciones Sanitarias, and a grant from Europharma (J.C.F.-C.). C.G.-R. and A.C. were partially supported by a grant from Europharma. A.M. is a Fellow from the Fondo Investigaciones Sanitarias.

ABBREVIATIONS: AA, antimycin A; BSO, buthionine L-sulfoximine; DCF, dichlorofluorescein; DCFDA, 2′-7′-dichlorofluorescin diacetate; DEM, diethylmaleate; GSH, reduced glutathione; MDA, malondialdehyde; ROS, reactive oxygen species; TTFA, thenoyltrifluoroacetone; NF-κB, nuclear factor-κB; HEPES, 4-(2-hydroxyethyl)-1-piperazineethanesulfonic acid; EMSA, electrophoretic mobility shift assay; DTT, dithiothreitol; EA, ethacrynic acid.

binding proteins to promoter *cis*-acting elements (6, 7). NF-κB is a well-studied pleiotropic, multisubunit transcription factor protein originally described as binding to an immunoglobulin κ enhancer site of B cells. Subsequently, a wide variety of inducible genes have been shown to contain κB binding sites in enhancer regions (8). NF-κB resides in the cytoplasm of different cell types as an inactive complex of the subunits p50 and p65 and an inhibitory subunit (IκB). The p50 and p65 subunits are the best-characterized members of a larger protein family (NF-κB/Rel/Dorsal). A wide variety of extracellular stimuli, including oxidative stress, lead to activation of NF-κB (9–13). NF-κB controls the inducible expression of various genes that are involved in immune responses as well as inflammatory and cellular defense mechanisms. Target genes of NF-κB include cytokines, cytokine receptors, and several viral enhancers that become up-regulated by the release of IκB with subsequent translocation of the p50-p65 heterodimer into the nucleus (9, 10).

Mitochondria from most mammalian cells do not contain catalase, implying that GSH in the mitochondrial matrix is the only defense available with which to cope with the potential toxic effects of hydrogen peroxide produced endogenously in the electron transport chain (5). The only known exception is heart, where the presence of catalase has recently been demonstrated, which might reflect a unique metabolism of hydrogen peroxide in this organ (14). It has long been known that the mitochondrial respiratory chain generates superoxide anion secondary to the interruption of electron flow between the rotenone- and antimycin-sensitive sites through one-electron reduction (5, 15–17). This mitochondrial-derived oxygen-activated species formation has been shown to be a contributory mechanism to the injury observed in several tissues during chemical hypoxia or ischemia/reperfusion (18–20). However, in these studies, the role of mitochondrial GSH was not examined. In addition, we know of no reported studies on the role of GSH in the maintenance of mitochondrial and extramitochondrial functions in a situation where oxidative stress is imposed by interference of electron flow in the respiratory chain in the absence of hypoxia or without the addition of exogenous oxidants. Thus, the purpose of the present study was to evaluate the modulation of mitochondrial GSH in the maintenance of mitochondrial function and activation of transcription factor NF-κB when the mitochondrial respiration chain at the complex III is inhibited to induce an endogenous oxidative stress.

Experimental Procedures

Materials. Coenzyme A, GSH, glutathione disulfide, EA, BSO, DEM, AA (mixture of antimycins A_1 and A_3), 2-heptyl-4-hydroxyquinoline-*N*-oxide, rotenone, TTFA, and sucrose were obtained from Sigma Chemical Co. (St. Louis, MO). ATP and DTT were purchased from Boeringher Mannheim (Mannheim, Germany). DCFDA and parinaric acid were obtained from Molecular Probes (Eugene, OR).

Isolation of rat liver mitochondria and hepatocytes and fractionation of hepatocytes. Rat liver mitochondria were isolated from liver homogenates (in 220 mM mannitol, 70 mM sucrose, 3 mM Tris·HCl, pH 7.4, containing 0.1 mM EDTA and 0.1% bovine serum albumin) by differential centrifugation (21). The final mitochondrial preparation was typically enriched in succinic dehydrogenase (3–4-fold) compared with homogenate and de-enriched in lactic dehydrogenase and oleoyl-CoA oxidase with oleoyl-CoA (200 μM), indicating the absence of cytosol and peroxisomes, respectively. Hepatocytes were isolated as described previously (22, 23). Initial cell viability was determined with the use of trypan blue. Time-dependent cell viability during the course of incubation of cells in the presence of AA was determined by either measurement in the medium of glutathione-*S*-transferase by the formation of 1-chloro-2,4-dinitrobenzene/GSH conjugate at 340 nm or trypan blue exclusion. Separation of cytosolic and mitochondrial compartments from isolated hepatocytes was accomplished through selective permeabilization of the plasma membrane with digitonin followed by centrifugation through an oil-mixture layer (silicon/paraffin, 6:1). The intact mitochondrial fraction was recovered at the bottom of the tube, whereas the cytosolic fraction was found at the top, with minimal cross-contamination (24). ATP levels from cells were determined by high performance liquid chromatography as previously described (22).

Mitochondrial respiration. Mitochondrial respiration was monitored with the use of a 1200-μl reaction vessel and a Clark oxygen electrode in respiration buffer (225 sucrose, 5 mM $MgCl_2$, 10 mM KH_2PO_4, 20 mM KCl, 10 mM Tris, and 5 mM HEPES, pH 7.4) using glutamate/malate or succinate as substrates for complex I or II. States 3 and 4 of respiration were determined in the presence or absence of ADP as described previously (23).

Depletion of mitochondrial GSH. GSH was depleted *in vitro* by preincubation of mitochondria or hepatocytes with DEM (0.2–0.8 mM) or EA (250 μM) for 10–15 min, followed by removal of the agent through washing. In other instances, *in vivo* depletion of GSH was accomplished through administration of BSO (3 mmol/kg/day i.p. in saline) for 4 days before isolation of mitochondria (25).

Determination of ROS. Production of ROS was monitored with a fluorescent probe, DCFDA, which oxidizes in the presence of hydrogen peroxide (26). Mitochondria (5–10 mg/ml) or hepatocytes (1–2 × 10^6 cells/ml in Krebs-Henseleit buffer) were incubated with the fluorescent probe (2 μM) in the absence or presence of AA (4 μl of an ethanolic stock solution of 15 mM). The mitochondrial suspension was incubated under room air for various periods of time. Fluorescence was determined at 529 nm for emission and 503 nm for excitation, with a slit width of 10 and 5 nm, respectively, according to the spectral characteristics of DCF. Spectra features of AA solution showed no emission maximum at 529 nm when excited at 503 nm. Preliminary experiments with isolated mitochondria indicated that the presence of AA did not interfere with the emission of fluorescence of DCF, with an emission maximum at 529 nm (not shown), which indicates that under these conditions the fluorescence of DCF was due to the formation of hydrogen peroxide and not to the presence of AA. The presence of ethanol as solvent for AA did not affect the spectra of DCF. Additional incubations included the presence of rotenone (15 μM) and TTFA (20 μM) to block complex I or II of the electron transport chain, respectively.

Measurement of lipid peroxidation. Lipid peroxidation was determined by MDA formation according to the method of Uchiyama and Mihara (27). Alternatively, lipid peroxidation was determined by quenching the fluorescence of parinaric acid as described previously (28). Mitochondrial or cell suspensions were incubated with parinaric acid at 5 μg/ml, and fluorescence was determined at 318 nm for excitation and at 410 nm for emission.

Determination of mitochondrial complex IV and ATPase. Complex IV of electron transport chain was determined by measuring the consumption of oxygen with the use of tetramethyl-*p*-phenylenediamine/ascorbate (0.2 mM/1 mM) as an artificial electron donor. Because experiments were done in the presence of AA, the electron flow from complex III to cytochrome *c* was inhibited. The F_1 component of ATPase activity was determined by linking ATP hydrolysis to NADH oxidation, as described previously (29).

Preparation of nuclear extracts. Nuclear extracts from hepatocytes were prepared according to Schreiber *et al.* (30) by lysing cells with Nonidet P-40 (0.25%) in 10 mM HEPES, pH 7.8, containing 10 mM KCl, 2 mM $MgCl_2$, 1 mM DTT, 0.1 mM EDTA, 0.1 mM phenyl-

methylsulfonyl fluoride, and 0.05 mg/ml aprotinin. Cells were vigorously mixed and centrifuged at 4° at 13,000 × *g*. Pelleted nuclei were resuspended in 50 μl with 50 mM HEPES, pH 7.8, containing 50 mM KCl, 300 mM NaCl, 1 mM DTT, 0.1 mM EDTA, 0.1 mM phenylmethylsulfonyl fluoride, 0.05 mg/ml aprotinin, and 10% glycerol. After gentle mixing for 20 min, supernatant resulting from spinning at 13,000 × *g* was collected and stored at −70°.

EMSAs. EMSAs were performed with the use of oligonucleotide probes encompassing the underlined binding site of NF-κB and Oct-1: NF-κB, 5′-AGT TGA *GGG GAC TTT CC*C AGG C-3′, 3′-TCA ACT CCC CTG AAA GGG TCC G-5′; Oct-1, 5′-TTC TAG T*GA TTT GCA* TTC GAC A-3′, 3′-AAG ATC ACT AAA CGT AAG CTG T-5′.

Probes were labeled at the 5′ end with T4 kinase and [γ-^{32}P]ATP (3000 Ci/mmol). Excess unreacted ATP was separated from the labeled probe through sequential ethanol precipitation. Binding reactions were performed according to Sen and Baltimore (8) and Fried and Crothers (31) and contained 3–5 μg nuclear protein, 1 μg poly(dI-dC), ^{32}P-labeled probe, 50 mM NaCl, 0.2 mM EDTA, 0.5 mM DTT, 2% glycerol, and 10 mM Tris·HCl, pH 7.5. Proteins were separated through native 6% polyacrylamide gel electrophoresis and visualized by autoradiography.

Statistical analysis. Statistical analyses for comparison of mean values for multiple comparisons between mitochondrial preparations were made by one-way analysis of variance followed by Fisher's exact test.

Results

Inhibition of complex III of the electron transport chain increases hydrogen peroxide. Peroxides can be detected through the use of the nonfluorescent dye DCFDA, which is freely permeable to membranes. Thereafter, it becomes hydrolyzed to 2′-7′-dichlorofluorescin. This precursor then interacts with peroxides and is oxidized to the fluorescent compound DCF. Emission spectra of AA solution in the absence of 2′-7′-dichlorofluorescin revealed a maximum emission at 503 nm when excited at 503 nm that was dependent on the dose of AA added (not shown). The addition of hydrogen peroxide did not affect the emission spectra of AA. However, on addition of 2′-7′-dichlorofluorescin, there was a maximum emission at 529 nm that was increased by the addition of hydrogen peroxide, demonstrating that the fluorescence observed at 529 nm with excitation at 503 nm was due to DCF and not to AA. Because the fluorescence of DCF is specific for detection of peroxides (18, 26), we related the fluorescence of DCF with the concentration of hydrogen peroxide, which was linear up to 150 μM of hydrogen peroxide (Fig. 1A), allowing us to determine the production of hydrogen peroxide by AA by measuring the fluorescence of the mitochondrial suspension in the presence of DCF and AA. The time course and dose-dependency of DCF production reflecting hydrogen peroxide generation in isolated mitochondria are shown in Fig. 1. Mitochondria were energized by succinate to drive electron flow through complex II. No significant increase of hydrogen peroxide was detected during as long as 2 hr of incubation. However, in the presence of AA, there was an increase in the production of hydrogen peroxide that was dependent on the dose of AA (1–15 μM or 0.2–3 nmol AA/mg protein) being linear up to 60 min of incubation (Fig. 1B). Greater concentrations of AA in the mitochondrial suspension led to fluorescence quenching of DCF, probably reflecting nonspecific effects of AA at concentrations of >3 nmol AA/mg protein (Fig. 1C). Therefore, we used AA at a dose of 3 nmol/mg protein in the incubations. Previous studies (17) have revealed a maximum capacity of mitochondria to generate superoxide anion at a similar range of AA (1–3 nmol/mg protein). Thus, our results obtained with AA at the highest dose maximally inhibited electron flow at complex III and oxygen uptake (Table 1), resulting in production of hydrogen peroxide. In addition, to discount possible nonspecific effects of AA produced under study conditions, we determined the effect of another complex III inhibitor, 2-heptyl-4-hydroxyquinoline-*N*-oxide (10–15 μM); results were similar to those obtained with AA (not shown). The maximum capacity of AA concentration in inducing ROS by mitochondria was related to its ability to block oxygen consumption (Table 1; 15 μM or 3 nmol/mg protein). That the increase in fluorescence of DCF detected with study assay conditions is not due to the presence of AA was indicated by the fact that mitochondrial suspension incubated with AA in the absence of DCFDA resulted in a fluorescence signal of 2–5% of that detected when DCFDA was added. By relating the fluorescence of DCF to the calibration curve, we determined the actual rate of production of hydrogen peroxide by mitochondria (0.33 and 2.3 nmol/min/mg protein in the absence and presence of AA, respectively) to be in the same range as previously described in isolated mitochondria with the use of different assays to detect hydrogen peroxide formation (Refs. 5 and 32, including citations).

To further support the view that inhibition of electron flow distal to the ubiquinone pool at complex III is the major producer of reactive oxygen intermediates, specifically hydrogen peroxide, we inhibited electron flow at complexes I and II with known blockers of electron transfer at these sites, i.e., rotenone and TTFA, separately or in combination. Mitochondria (energized with glutamate/malate and succinate and incubated with rotenone and/or TTFA) did not exhibit significant increased production of hydrogen peroxide (Fig. 2). However, inhibition of electron flow at complexes I and II significantly prevented the increase of DCF production resulting from blockade of electron flow at complex III with AA. Although complex I also is a potential source of superoxide anion, its capacity to produce hydrogen peroxide is lower than that of complex III. The ability of rotenone to partially block AA-induced hydrogen peroxide production by mitochondria is in agreement with previous described studies (17).

DCF production within the electron transport chain is controlled by availability of GSH. Because hydrogen peroxide is a product of oxygen activation within the electron transport chain, its detoxification could be controlled by defense systems found in mitochondria. Preincubation of mitochondria with DEM or EA led to depletion of GSH levels (Fig. 3A, *inset*). This resulted in a significant increase in DCF after 60 min (Fig. 3A). However, inhibition of complex III by AA in mitochondria that were depleted of GSH potentiated the increase of DCF compared with the addition of AA in mitochondria with repleted GSH levels (Fig. 3A). To rule out nonspecific effects of EA or DEM pretreatment of mitochondria, we depleted mitochondrial GSH *in vivo* using a selective inhibitor of GSH synthesis and therefore of mitochondrial GSH, i.e., BSO. Administration of BSO to rats resulted in a significant 40–50% mitochondrial GSH depletion compared with rats injected with saline (Fig. 3B, *inset*). Mitochondria from BSO-treated animals showed greater DCF fluorescence than saline-injected control animals. Incubation of mitochon-

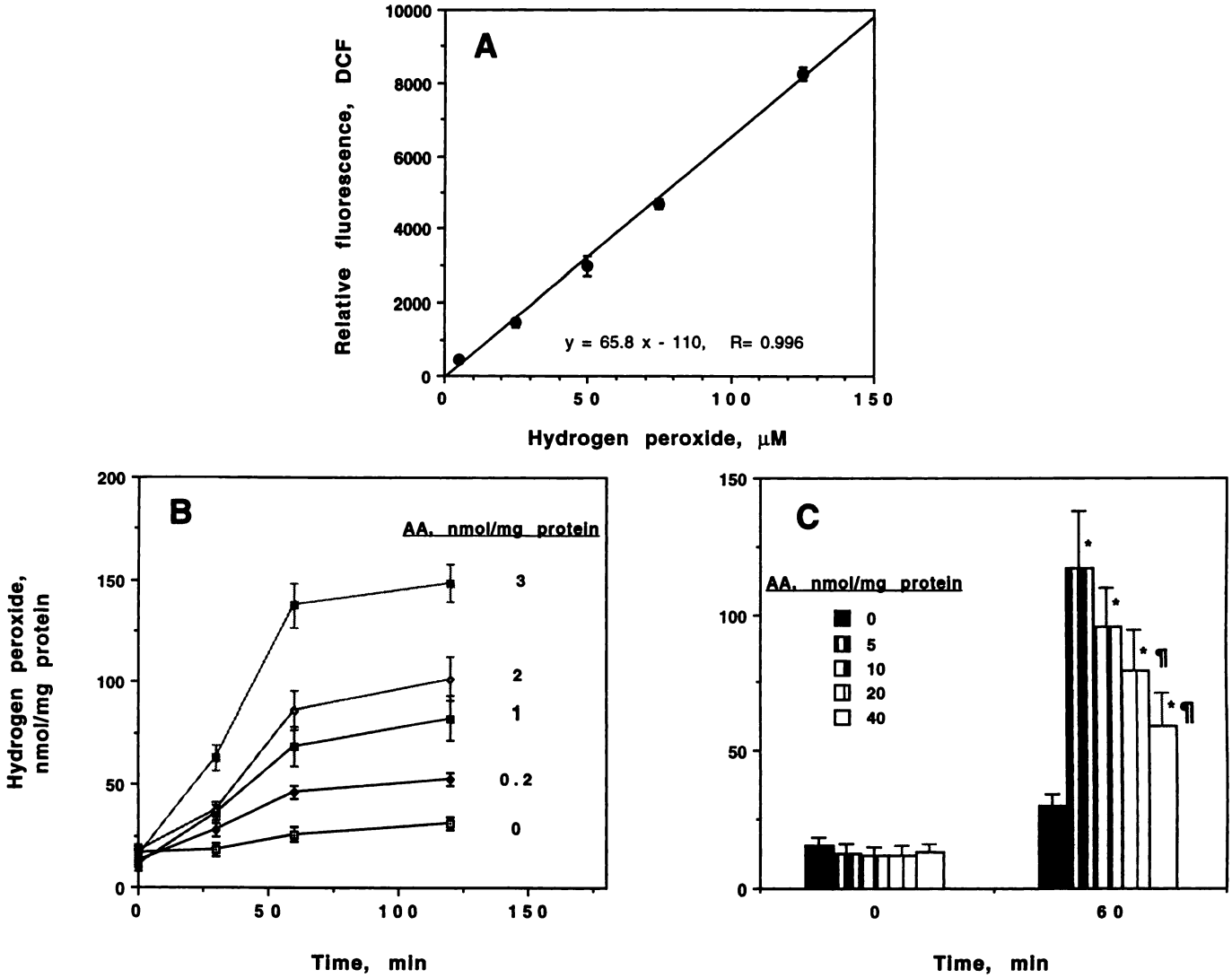

Fig. 1. Time course and dose-dependence of hydrogen peroxide production in isolated mitochondria treated with AA. A, Correlation between fluorescence of 2′-7′-dichlorofluorescein in the presence of increasing concentrations of hydrogen peroxide. Fluorescence was determined with excitation at 503 nm and emission at 529 nm. B, Mitochondria (5–10 mg/ml) were incubated with AA (0.2–3 nmol/mg protein) and DCFDA (2 μM) to detect hydrogen peroxide production by fluorescence of DCF. At various times of incubation, aliquots were transferred to a fluorimetric cuvette, and production of DCF was determined as described in Experimental Procedures. C, Hydrogen peroxide production determined as DCF fluorescence of mitochondria incubated with the indicated doses of AA for 60 min. Results are given as mean ± standard deviation for four cell preparations. *, $p < 0.05$ versus the absence of AA; ¶, $p < 0.05$ versus the presence of AA (5 nmol/mg).

dria from BSO-treated animals with AA resulted in a greater increase in DCF (Fig. 3B). However, this degree of DCF production by AA in BSO-treated animals was not as great as that observed after *in vitro* incubation of mitochondria with EA. Because these maneuvers resulted in a wide range of initial GSH levels, we sought to relate the production of DCF by AA to the starting GSH of mitochondria. As observed in Fig. 4, there was a dependence of DCF production on the level of GSH in mitochondria. Depletion of mitochondrial GSH below a critical level of 3 nmol/mg protein resulted in significant increased production of DCF by AA. Without AA, increased DCF production was seen at lower mitochondrial GSH levels (<1 nmol/mg protein). DCF was not a substrate for glutathione-*S*-transferase, suggesting that the decline of fluorescence of DCF at high mitochondrial GSH concentrations cannot be explained by limited availability of the fluorescent probe to oxidization by hydrogen peroxide (not shown).

Increased production of ROS by AA results in lipid peroxidation and loss of mitochondrial functions. Lipid peroxidation is one of the manifestations of excessive production of prooxidants. We determined lipid peroxidation by MDA production. Increased generation of hydrogen peroxide within mitochondria by AA resulted in significant production of MDA (Figs. 3 and 5). Depletion of mitochondrial GSH by EA, DEM, or BSO resulted in greater production of MDA. Incubation of mitochondria with EA or DEM in the absence of AA did not result in toxic manifestations as seen by maintenance of coupled respiration for the period of observation (not shown). Incubation with AA of mitochondria depleted of GSH by these agents led to a further potentiated increase in MDA (Fig. 5). Similar results were obtained when lipid peroxidation was determined fluorimetrically with parinaric acid (not shown). To evaluate the impact of generation of ROS on functional activities of mitochondria, we determined the activity of the F_1 component of the ATPase com-

TABLE 1

Oxygen consumption of mitochondria and isolated hepatocytes and effect of respiratory inhibition

Oxygen consumption rates at different states were induced by addition of succinate with or without ADP and oxygen consumption was determined polarographically with an Oxygraph (Gilson Electronics) equipped with oxygen clark-electrode. Data represent the end of a 60-min incubation of mitochondria in the absence of AA. States 4 and 3 of respiration at the beginning of incubation were 22.7 ± 3.4 and 137.1 ± 18 nmol/min/mg protein, respectively. The effect of AA on the oxygen consumption was determined at different dose of the blocker of complex III in the absence of ADP.

Mitochondria	Oxygen consumption
	nmol O_2/min/mg protein
State 4	19.1 ± 3.1
State 3	123 ± 16
AA dose	
(nmol/mg protein)	
0	23.2 ± 2.1
0.2	11.2 ± 1.2
1	4.6 ± 1.1
2	0.6 ± 0.4
3	0.2 ± 0.1
Hepatocytes	
AA dose	
(nmol/10^6 cells)	*nmol/min/10^6 cells*
0	19.7 ± 1.2
0.5	14.1 ± 0.9
2.5	7.2 ± 0.3
5	1.3 ± 0.2
7.5	0.6 ± 0.1

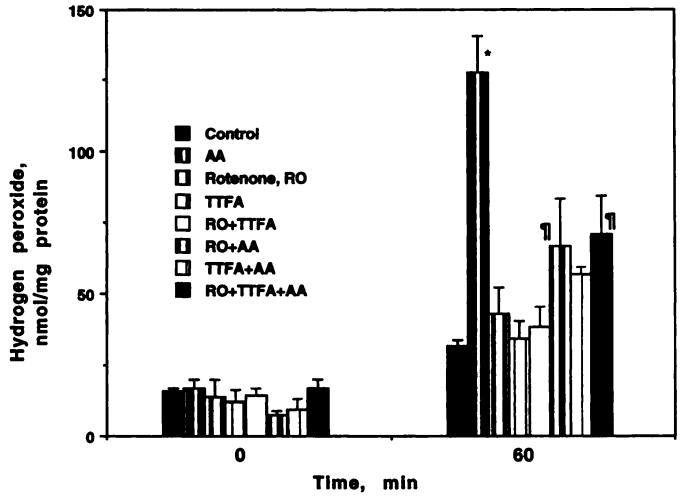

Fig. 2. Hydrogen peroxide production of mitochondria after inhibition of electron flow at complexes I, II, and III of the electron transport chain. Mitochondria were incubated in the presence of rotenone (20 μM), TTFA (15 μM), and AA (15 μM, 3 nmol/mg protein). For the combination of the three inhibitors, mitochondria were preincubated with rotenone/TTFA for 15 min before the addition of AA to the mixture. After 60 min of incubation, DCF was detected as described in Experimental Procedures. Results are given as mean ± standard deviation of four cell preparations. *, $p < 0.05$ versus control; ¶, $p < 0.05$ versus AA.

plex and the consumption of oxygen at the complex IV segment of the electron transport chain. As shown in Fig. 6, incubation of mitochondria with AA did not result in reduction in ATPase compared with mitochondria not treated with AA. However, depletion of mitochondrial GSH *in vivo* through treatment with BSO or *in vitro* through preincubation of mitochondria with EA led to a significant loss of activity of both functional mitochondrial parameters in the presence of AA (Fig. 6). Although *in vivo* BSO treatment

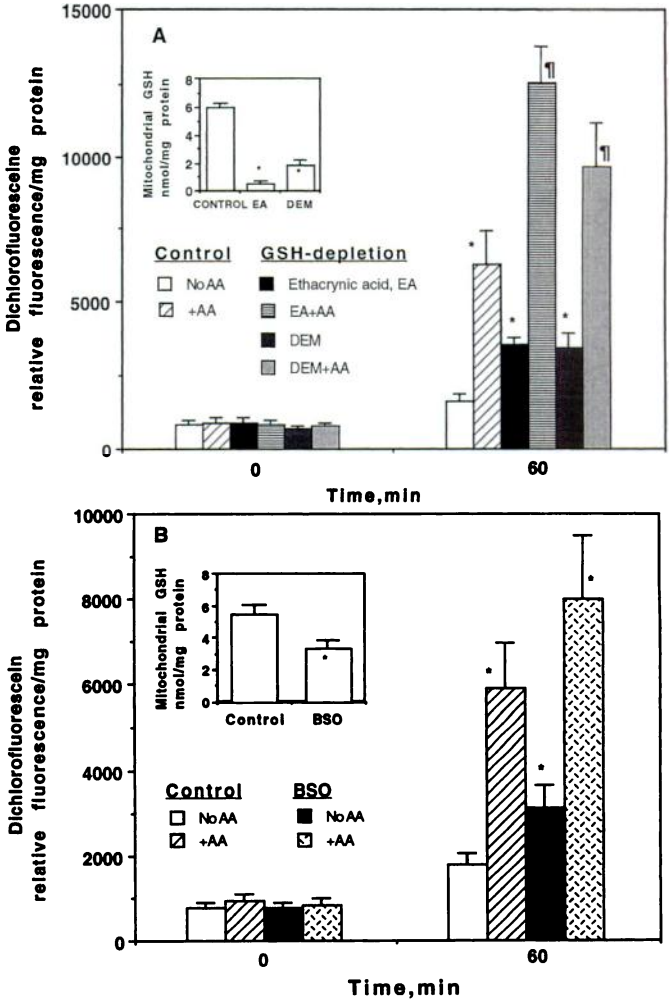

Fig. 3. Production of DCF by AA at different levels of mitochondrial GSH. A, *In vitro* depletion of GSH was accomplished through incubation of mitochondria with EA (250 μM) or DEM (0.8 mM) for 15 min followed by washing of mitochondria. B, *In vivo* depletion was performed by treating rats with BSO as described in Experimental Procedures. *Control*, mitochondria not depleted of GSH. *Inset*, starting mitochondrial GSH levels before incubation with AA. After GSH depletion, mitochondria were incubated with AA (15 μM) for 60 min, and DCF fluorescence was determined as described in Experimental Procedures. Results are given as mean ± standard deviation of four cell preparations. *, $p < 0.05$ versus control in the absence of AA. ¶, $p < 0.05$ versus control in the presence of AA.

resulted in less quantitative mitochondrial GSH depletion than *in vitro* incubation of mitochondria with DEM or EA, it reached depletion below a critical level that resulted in alteration of mitochondrial function by AA. Similar results were obtained when mitochondrial GSH depletion was induced by DEM pretreatment *in vitro* (not shown). States 3 and 4 of mitochondrial respiration remained stable during the 60-min incubation period, indicating that our results regarding mitochondrial function were not the consequence of nonspecific loss of mitochondrial functions (Table 1).

Increased production of ROS and activation of NF-κB by AA treatment in GSH-depleted hepatocytes. In isolated hepatocytes, selective depletion of either cytosolic or both cytosolic and mitochondrial GSH can be accomplished through incubation of cells with different doses of DEM (24). Incubation of cells with 0.2 mM DEM resulted in a rather

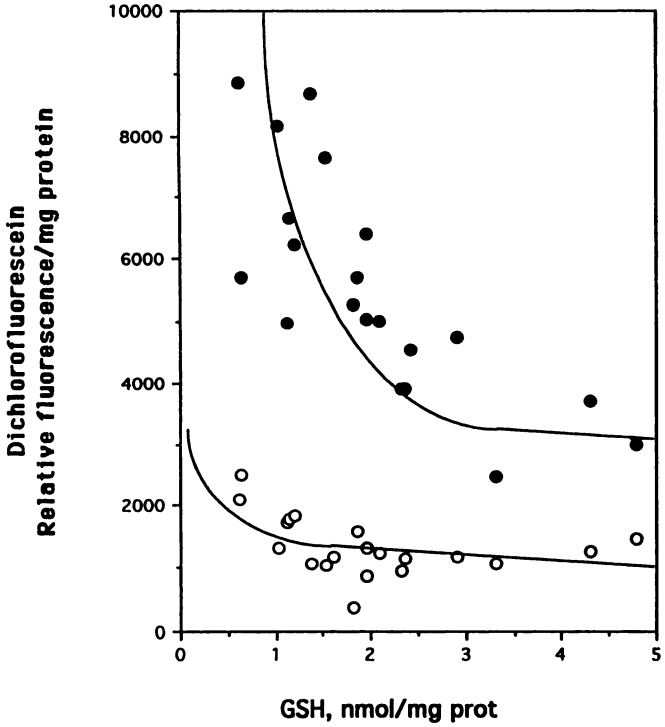

Fig. 4. Dependence of DCF production on mitochondrial GSH. A wide range of mitochondrial GSH levels were achieved through *in vitro* treatment of mitochondria with various doses of DEM or EA or through isolation of mitochondria from rats pretreated with BSO. Mitochondria were then incubated in the presence (*filled symbols*) and absence (*open symbols*) of 15 μM AA (3 nmol/mg protein) for 60 min, and DCF was determined as described in Experimental Procedures. *Solid line*, fit to the data by polynomial equation up to 3 nmol of GSH/mg protein and 1 nmol/mg protein and linearly from 3–5 nmol/mg protein and 1–5 nmol/mg protein for cells in the presence or absence of AA, respectively. DCF in the presence of AA was statistically significantly greater than in the absence of AA at all GSH concentrations.

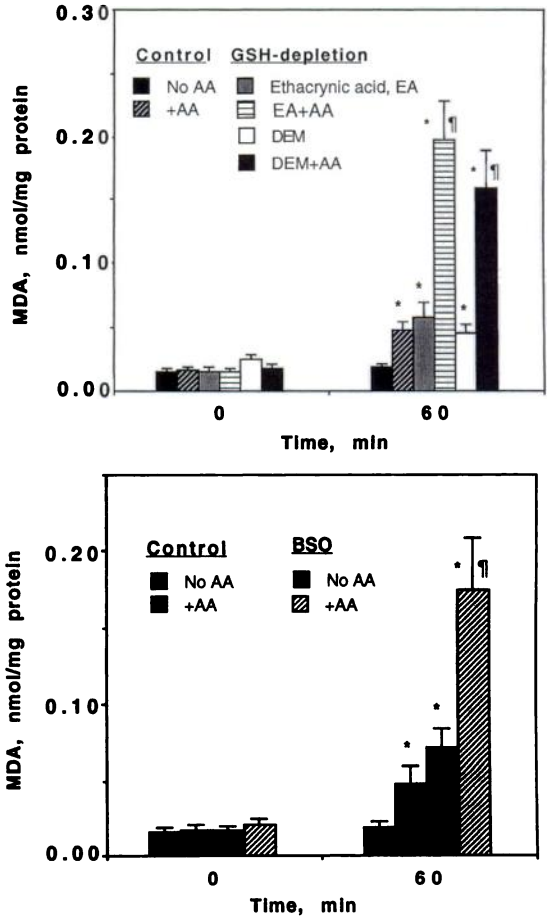

Fig. 5. AA-induced mitochondrial lipid peroxidation. Lipid peroxidation was determined as MDA formed during 60 min of incubation of mitochondria with AA. See Fig. 3 legend for description of conditions used to deplete GSH. Results are given as mean ± standard deviation of four cell preparations. *, $p < 0.05$ versus the absence of AA. ¶, $p < 0.05$ versus the corresponding value without AA.

selective depletion of cytosolic GSH by 80%, whereas the mitochondrial pool of GSH was depleted by 20% of control (Fig. 7). In contrast, 0.8 mM DEM led to 92% and 88% depletion of cytosolic and mitochondrial GSH, respectively. Under these circumstances, exposure of cells to AA increased the fluorescence of DCF, an increase that was greater in cells severely depleted of mitochondrial GSH (Table 2). This response was accompanied by greater lipid peroxidation in the form of MDA or loss of parinaric fluorescence and decrease in complex IV of respiration during the incubation of cells with AA. However, there was no significant change in cell viability under these various conditions up to 60 min of incubation, although extended incubation in the presence of AA indicated a greater vulnerability of cells pretreated with 0.8 mM DEM compared with 0.2 mM DEM (Table 3). Blockade of complexes I and II by rotenone and TTFA protected against killing of cells by AA (Table 3).

Because NF-κB is a transcription factor that becomes activated in the nucleus of cells exposed to prooxidant conditions (9–12), we next investigated the activation of NF-κB in response to AA in cells that were pretreated with DEM. First, we determined the presence in cytosol of hepatocytes of an inducible NF-κB. Activation of inactive cytosolic NF-κB can be achieved through treatment with detergents that dissociate IκB from the DNA-binding competent heterodimer. Deoxycholate pretreatment of cytosol resulted in the presence of a band detected by EMSA that was completely displaced when binding assays were performed in the presence of a molar excess of unlabeled NF-κB (Fig. 8A). We determined the degree of activation of NF-κB by AA and the influence of severe depletion of mitochondrial and cytosolic GSH versus selective depletion of cytosolic GSH. Nuclear extracts of cells pretreated with DEM were obtained after incubation with AA for 10 min. AA treatment resulted in the presence of a retarded band that was displaced by excess unlabeled NF-κB. The pattern of activation of NF-κB by AA treatment of cells preincubated with 0.2 mM DEM was greater than that in cells not treated with DEM but less than that in cells pretreated with 0.8 mM DEM (Fig. 8, B and C). The activation of NF-κB under these circumstances was paralleled by greater production of DCF compared with cells not treated with DEM (Fig. 8D). Nuclear extracts from cells pretreated with rotenone and TTFA before exposure to AA did not exhibit an increase in DCF and activation of NF-κB (not shown).

We next determined the time course of activation of NF-κB and DCF production by AA in response to DEM pretreatment of hepatocytes. As seen in Fig. 9, nuclear extracts from cells incubated with AA led to activation of NF-κB that was maximal at 15 min of incubation with AA (Fig. 9A). However, the addition of AA to cells that were preincubated with 0.8 mM

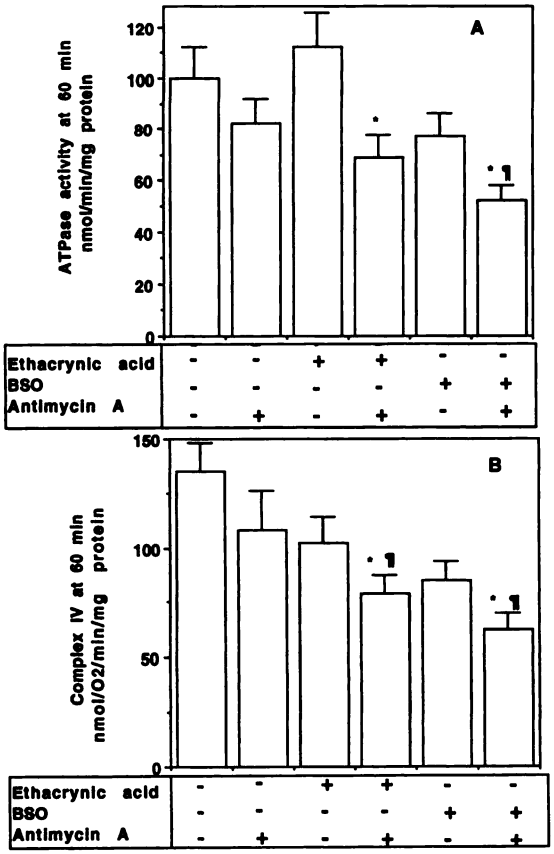

Fig. 6. Effect of AA with or without GSH depletion on mitochondrial function. ATPase activity (A) and complex IV respiration (B) were determined in mitochondria pretreated with EA or BSO to induce *in vitro* or *in vivo* GSH depletion as in Fig. 3. Results are given as mean ± standard deviation of three cell preparations. *, $p < 0.05$ versus the absence of AA. ¶, $p < 0.05$ versus the presence of AA in mitochondria not depleted of GSH.

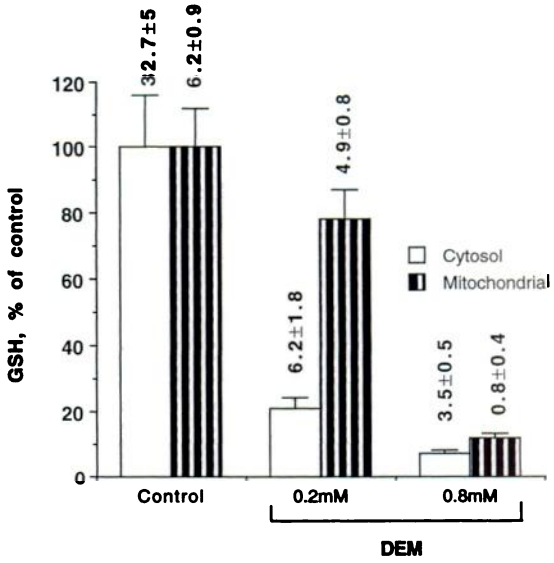

Fig. 7. Depletion of cytosolic or mitochondrial GSH of hepatocytes by DEM. Hepatocytes were incubated with 0.2 or 0.8 mM DEM for 15 min. Cells were then washed and fractionated into cytosol and mitochondria (24). GSH was determined in either compartment by high performance liquid chromatography. Results are given as percentage of untreated control values. Numerical values refer to GSH levels expressed as nmol/10^6 cells. Results are given as mean ± standard deviation of five cell preparations. $p < 0.05$ for cytosol depletion by 0.2 mM DEM versus control hepatocytes.

DEM resulted in earlier activation of NF-κB, peaking at 5 min of incubation with AA. This pattern of activation was mirrored by the increase in DCF by AA (Fig. 9B). In contrast, Oct-1, a constitutive transcription factor, was not activated in response to AA or GSH depletion (Fig. 9A). Interestingly, the activation of NF-κB declined under both conditions at 30 min of incubation with AA, despite maintenance of increased levels of DCF up to 30 min of incubation. Although the specific pattern of activation of this transcription factor varies among cell types, similar transient activation has been obtained in other cell types exposed to prooxidants such as hydrogen peroxide, lipopolysaccharide, or phorbol-12-myristate-13-acetate (12, 33). This transient activation has also been observed not only in relation to time but also in relation to the dose of hydrogen peroxide exposure.

Discussion

Most oxygen consumption in mitochondria occurs at cytochrome *c* oxidase, where dioxygen undergoes a four-electron reduction to 2 molecules of water. In this process, dioxygen is tightly bound to the heme group of cytochrome a_3, and electrons are transferred with no release of partially reduced oxygen intermediates. The present studies are based on previous observations on isolated mitochondria showing that molecular oxygen can undergo a one-electron reduction, with formation of superoxide anion and hydrogen peroxide (5, 15–17). Recent studies have provided evidence that oxidative phosphorylation is a source of oxygen radicals in both cell suspension and intact organs, suggesting that mitochondrial respiration might be an important contributor to the pathogenesis of reperfusion injury (18–20). The results of the present study have extended these previous reports to determine the importance of mitochondrial GSH in controlling both mitochondrial and extramitochondrial functional consequences of an oxidative stress arising in mitochondria as generated by the interruption of mitochondrial respiration at complex III. To our knowledge, there have been no previous reports specifically aimed at this issue. Our results confirm that the one-electron transfer of ubisemiquinone to oxygen at complex III can induce endogenous oxidative stress in mitochondria because inhibition of complex III by AA results in increased production of hydrogen peroxide. In addition, blockade of other segments of the respiratory chain, such as complexes I and II of respiration, not only did not result in increased generation of ROS but also prevented the AA-induced formation of hydrogen peroxide. This outcome is similar to what has been previously reported for submitochondrial particles incubated with rotenone and antimycin (17).

Oxidative stress can be viewed as an imbalance between prooxidants and antioxidants. Increased production of reactive oxygen intermediates or decreased availability of the defenses that detoxify and protect against them result in endogenous oxidative stress. The GSH redox system is the only way mitochondria can maintain a low steady state concentration of hydrogen peroxide, which is being constantly formed as a result of mitochondrial respiration because mitochondria from most cells do not contain catalase (4, 5, 14). Our data clearly show that GSH within the mitochondrial

TABLE 2

DCF, MDA, and complex IV respiration in hepatocytes treated with AA

Results were obtained after 60 min of incubation of cells (2×10^6 cells, 5 ml, Krebs-Henseleit buffer) with 15 μM AA. Results are expressed as relative fluorescence of DCF and nmol of MDA produced per 1 million cells. Complex IV was measured polarographically by addition of ascorbate and TMPD as described in Experimental Procedures. Initial values of GSH in cytosol and mitochondria achieved after preincubation of cells with DEM for 15 min are shown in Fig. 7. Initial values of DCF, MDA, and complex IV are 789 ± 123 fluorescence/10^6 cells, 0.010 ± 0.001 nmol/10^6 cells, and 173 ± 22 nmol O_2/min/mg protein, respectively. Values in the presence of AA are statistically different compared with absence of AA.

Condition	DCF		MDA		Complex IV	
	−AA	+AA	−AA	+AA	−AA	+AA
Control	1989 ± 312	9456 ± 934	0.012 ± 0.003	0.052 ± 0.008	165 ± 21	131 ± 17
0.2 mM DEM	2876 ± 437	11424 ± 1032[a]	0.041 ± 0.006	0.081 ± 0.01[a]	148 ± 18	119 ± 16
0.8 mM DEM	5345 ± 654	15676 ± 1767[b]	0.062 ± 0.008	0.189 ± 0.02[b]	151 ± 19	106 ± 21[a]

Results are mean ± standard deviation of three to five cell preparations.
[a] $p < 0.05$ versus control cells +AA.
[b] $p < 0.05$ versus 0.2 mM DEM cells +AA.

TABLE 3

Time-dependent viability of hepatocytes exposed to AA

Results represent viability determined by GST activity found in medium of cells incubated with 15 μM AA for the indicated period of time or by trypan blue obtaining similar results. Starting GSH levels in cytosol and mitochondria are shown in Fig. 7. Initial cell viability did not differ between different cell groups 87–91%.

Condition	60 min		120 min		
	−AA	+AA	−AA	+AA	+AA + rotenone + TTFA
Control	85 ± 7	82 ± 6	80 ± 8	79 ± 8	78 ± 7
0.2 mM	83 ± 6	81 ± 5	82 ± 8	62 ± 7[a]	72 ± 5
0.8 mM	81 ± 7	79 ± 7	75 ± 7	44 ± 7[ab]	69 ± 4

[a] $p < 0.05$ versus control cells +AA.
[b] $p < 0.05$ versus 0.2 mM DEM cells +AA.

matrix is critical not only in the direct detoxification of hydrogen peroxide but also in interrupting the sequence of reactions that lead to hydroxyl radical formation from superoxide anion and hydrogen peroxide. In accord with this, our results demonstrated that the availability of ROS generated within the electron transport chain is controlled by matrix GSH, so depletion of mitochondrial GSH below a critical value results in significant potentiated production of ROS by AA as reflected in DCF and production of lipid peroxidation as MDA. However, despite direct evidence of production of hydrogen peroxide in these circumstances, this species might not be solely responsible for mitochondrial lipid peroxidation and loss of functions because hydroxyl radicals or other hydrogen peroxide-derived oxidants might have been formed through the participation of transition metals. In keeping with this, we observed that pretreatment of mitochondria with desferrioxamine before exposure to AA partially prevented lipid peroxidation and loss of mitochondrial functions without a significant effect on the production of DCF (not shown).

Our observations with isolated mitochondria have been confirmed in isolated hepatocytes. In addition, this system allowed us to examine the relative importance of mitochondrial and cytosolic GSH pools when faced with hydrogen peroxide production in mitochondria. Cells with marked depletion of cytosolic GSH in the presence of an intact pool of mitochondrial GSH show moderate consequences of oxidative stress imposed by the generation of ROS within the mitochondria, as reflected in lipid peroxidation, production of DCF, and activation of NF-κB, compared with cells not depleted of GSH. However, these manifestations of oxidative stress were markedly enhanced when the pool of mitochondrial GSH was diminished to <20% of control cells. Cells depleted of mitochondrial GSH were much more sensitive to the effects of excessive production of ROS, including lipid peroxidation, loss of mitochondrial complex IV activity, and activation of transcription factor NF-κB. In addition, increased vulnerability of these cells was demonstrated by the increased cell killing by AA when both mitochondrial and cytosolic GSH levels were depleted compared with selective depletion of cytosolic GSH. Hepatocytes not depleted of GSH were fairly resistant to cell killing by AA. However, prolonged exposure of cells to AA alone eventually resulted in cell killing at 2–3 hr compared with the absence of AA. However, by 60 min of incubation of cells with AA, ATP levels were lower (12.7 ± 1.3 versus 21.4 ± 3.7 nmol/10^6 cells) compared with cells in the absence of AA, but this ATP depletion was the same after preincubation with DEM to deplete the mitochondrial pool of GSH. Thus, in this paradigm, the loss of cell viability induced by AA might not necessarily be due to limited ATP availability to support cell functions but probably was caused by the mitochondrial oxygen radical formation by complex III of respiration. Furthermore, blockade of complexes I and II prevented killing by AA plus mitochondrial GSH depletion, which supports the critical role of excess hydrogen peroxide rather than impaired ATP synthesis. These findings confirm and support the importance of mitochondrial GSH in maintaining functional competent mirochondrial and cell viability (24, 34–37). Alternatively, contribution to the production of ROS by calcium should also be considered because the inner mitochondrial membrane may become very sensitive to the noxious effects of calcium when the mitochondrial reducing power (GSH, NADH) becomes limited (38, 39). However, this issue is related to the steps in cell killing that are enhanced by the combination of AA and mitochondrial GSH depletion. Thus, our data do not address whether the enhanced hydrogen peroxide exerts its toxicity by promoting lipid peroxidation or eliminating the reducing equivalents that modulate calcium effects.

Our study has demonstrated a previously unrecognized effect of mitochondrial oxidative stress and mitochondrial GSH defense on transcription factor activation. Our data not only provide evidence for the importance of GSH in maintaining vital mitochondrial functions but also suggest that GSH status in mitochondria may influence nuclear gene regulation. Oxygen intermediates may act as signal transducers and represent a versatile cellular control mechanism for gene regulation. Recent evidence has shown that activation and

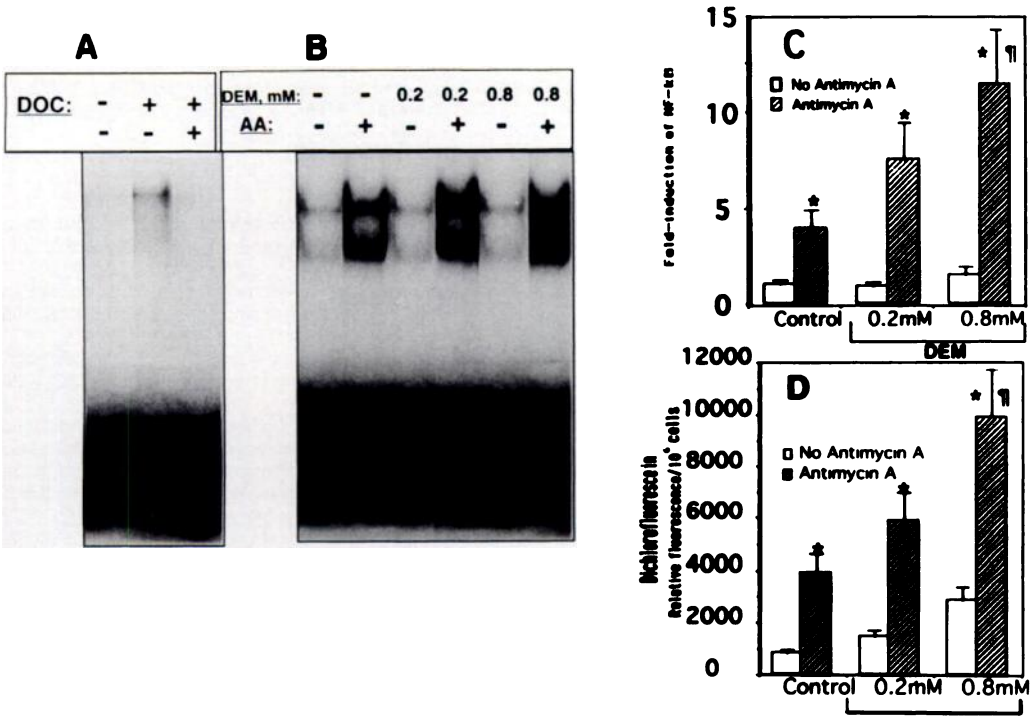

Fig. 8. Induction of NF-κB by AA. Hepatocytes were treated with AA for 10 min after preincubation with DEM (0.2 mM and 0.8 mM). Starting GSH levels are given in Fig. 7. A, EMSA of inducible NF-κB. Cytosol was treated with 1% sodium deoxycholate before the addition of labeled oligonucleotide probe for NF-κB. To verify specificity of induction, the binding mixture was incubated with excess (100-fold) unlabeled NF-κB. B, Activation of NF-κB by AA is dependent on the starting cytosolic and mitochondrial GSH levels of hepatocytes treated with AA. C, Fold induction of NF-κB by AA from cells pretreated with DEM. D, DCF formation of hepatocytes incubated with AA. *, $p < 0.05$ versus no AA. ¶, $p < 0.05$ versus AA at 0.2 mM DEM. Results are given as mean ± standard deviation of three cell preparations.

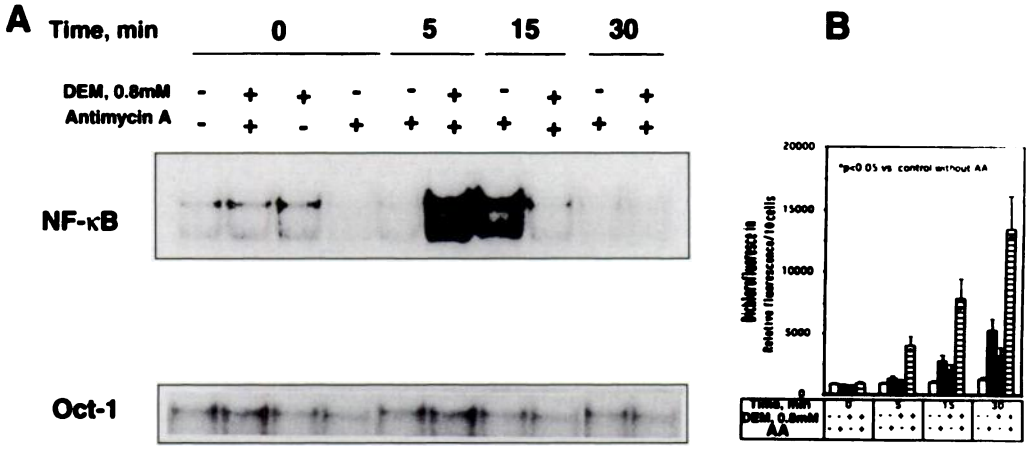

Fig. 9. Time-dependent increase of NF-κB by AA. Hepatocytes were incubated with AA with or without pretreatment with DEM. A, Representative EMSA using oligonucleotide probe for NF-κB and Oct-1. B, Time-dependent production of DCF under the same conditions. Results are given as mean ± standard deviation of three cell preparations. *, $p < 0.05$ versus no AA.

DNA binding of several transcription factors depend on the cellular redox state (13, 40–42). Specifically, recent observations have shown that mitochondrial electron transport is required for the activation of NF-κB and subsequent gene induction by tumor necrosis factor-α. However, this study did not address the role of mitochondrial GSH (40). Thus, because mitochondria are a major source of ROS in cells and because GSH in mitochondria controls the basal tone of ROS generated in the respiratory chain, mitochondrial GSH, by controlling the availability of the ROS, may affect nuclear gene regulation. We have shown that depletion of both cytosolic and mitochondrial GSH in hepatocytes results in greater activation of NF-κB than in cells depleted of only cytosolic GSH. In the present study, GSH depletion of mitochondria produced oxidative stress that was insufficient to impair mitochondrial function, and activation of NF-κB. AA alone was able to produce sufficient oxidative stress to impair mitochondrial function and activation of NF-κB. Because inhibition of complexes I and II prevented these effects of AA, our results suggest that oxidative stress originating in mitochondria was directly responsible for activation of NF-κB in intact cells. Depletion of mitochondrial GSH markedly accentuated the effect of AA on mitochondrial function and NF-κB. Thus, in disease states and tissue injury where increased oxidant stress occurs in mitochondria (e.g., ischemia-reperfusion, chronic ethanol ingestion, tumor necrosis factor-α-induced cytotoxicity associated with inflammatory response, programmed cell death; Refs. 24, 40, and 43–46), mitochondrial GSH status will be critical in determining loss of mitochondrial function and cell viability as well as transcription factor activation and gene regulation. Mitochondrial GSH depletion will accentuate these effects, whereas repletion will minimize them.

References

1. Ames, B. N., M. K. Shigenaga, and T. M. Hagen. Oxidants, antioxidants and the degenerative disease of aging. *Proc. Natl. Acad. Sci. USA* **90**:7915–7922 (1990).
2. Stadtman, E. R. Protein oxidation and aging. *Science (Washington D. C.)* **257**:1220–1224 (1992).
3. Shigenaga, M. K., T. M. Hagen, and B. N. Ames. Oxidative damage and

mitochondrial decay in aging. *Proc. Natl. Acad. Sci. USA* **91**:10771–10778 (1994).
4. Cerrutti, P. A. Prooxidant states and tumor promotion. *Science (Washington D. C.)* **227**:375–379 (1985).
5. Chance, B., H. Sies, and A. Boveris. Hydroperoxide metabolism in mammalian organs. *Physiol. Rev.* **59**:527–605 (1979).
6. McKnight, S., and R. Tjian. Transcriptional selectivity of viral genes in mammalian cells. *Cell* **46**:795–805 (1986).
7. Jonshon, P. F., and S. L. McKnight. Eukaryotic transcriptional regulatory proteins. *Annu. Rev. Biochem.* **58**:799–839 (1989).
8. Sen, R., and D. Baltimore. Multiple nuclear factors interact with immunoglobin enhancer sequences. *Cell* **46**:705–716 (1986).
9. Droge, W., K. Schulze-Osthoff, S. Mihm, D. Galter, H. Schenk, H.-P. Eck, S. Roth, and H. Gmünder. Functions of glutathione and glutathione disulfide in immunology and immunopathology. *FASEB J.* **8**:1131–1138 (1994).
10. Liou, H. C., and D. Baltimore. Regulation of NF-κB/rel transcription factor and IκB inhibition system. *Curr. Opin. Cell Biol.* **5**:477–491 (1993).
11. Grimm, S., and P. Bauerle. The inducible transcription factor NF-κB: structure-function relationship of its protein subunits. *Biochem. J.* **290**: 297–311 (1993).
12. Meyer, M., R. Schreck, and P. Bauerle. Hydrogen peroxide and antioxidants have opposite effects on activation of NF-kB and AP-1 in intact cells: AP-1 as secondary antioxidant responsive factor. *EMBO J.* **12**:2005–2011 (1993).
13. Staal, F. J. T., M. Roederer, L. A. Herzenberg, and L. A. Herzenberg. Intracellular thiols regulate activation of nuclear factor NF-κB and transcription of human imunodeficiency virus. *Proc. Natl. Acad. Sci. USA* **87**:9943–9947 (1990).
14. Radi, R., F. Turrens, L. Y. Chang, J. D. Bush, J. Crapo, and B. A. Freeman. Detection of catalase in rat heart mitochondria. *J. Biol. Chem.* **266**:22028–22034 (1991).
15. Loschen, G., L. Flohe, and B. Chance. Respiratory chain linked hydrogen peroxide formation in pidgeon heart mitochondria. *FEBS Lett.* **18**:261–264 (1971).
16. Turrens, J. F., A. Alexandre, and A. L. Lehninger. Ubisemiquinone is the electron donor for superoxide formation by complex III of heart mitochondria. *Arch. Biochem. Biophys.* **237**:408–411 (1985).
17. Turrens, J. F., and A. Boveris. Generation of superoxide anion by the NADH dehydrogenase of bovine heart mitochondria. *Biochem. J.* **191**:421–427 (1980).
18. Dawson, T., G. J. Gores, A.-L. Nieminen, B. Herman, and J. J. Lemasters. Mitochondria as a source of reactive oxygen species during reductive stress in rat hepatocytes. *Am. J. Physiol.* **264**:C961-C967 (1993).
19. Ambrosio, G., J. L. Zweier, C. Duilio, P. Kuppusany, G. Santoro, P. P. Elia, I. Tritto, P. Cirillo, M. Condorelli, M. Chiariello, and J. T. Flaherty. Evidence that mitochondrial respiration is a source of potentially toxic oxygen free radicals in intact rabbit hearts subjected to ischemia and reflow. *J. Biol. Chem.* **268**:18532–18541 (1993).
20. Hess, M. L., and N. H. Manson. Molecular oxygen: friend and foe. The role of oxygen-radical system in the calcium paradox, the oxygen paradox and ischemia reperfusion injury. *J. Mol. Cell. Cardiol.* **16**:969–978 (1984).
21. Schnaitman, C. A., and J. W. Greenawalt. Enzymatic properties of the inner and outer membranes of rat liver mitochondria. *J. Cell. Biol.* **33**: 158–175 (1968).
22. Fernández-Checa, J. C., C. Ren, T. Y. Aw, M. Ookhtens, and N. Kaplowitz. Effect of membrane potential and cellular ATP on glutathione efflux from isolated rat hepatocytes. *Am. J. Physiol.* **255**:G403–G408 (1988).
23. García-Ruiz, C., A. Morales, A. Ballesta A., J. Rodes, N. Kaplowitz, and J. C. Fernández-Checa. Effect of chronic ethanol feeding on glutathione and functional integrity of mitochondria in periportal and perivenous rat hepatocytes. *J. Clin. Invest.* **94**:193–201 (1994).
24. Fernández-Checa, J. C., C. García-Ruiz, M. Ookhtens, and N. Kaplowitz. Impaired uptake of glutathione by hepatic mitochondria from ethanol-fed rats. *J. Clin. Invest.* **87**:397–405 (1991).
25. Martensson, J., A. Jain, E. Stole, W. Frayer, P. Auld, and A. Meister. Inhibition of glutathione synthesis in the newborn rat: a model for endogenously produced oxidant stress. *Proc. Natl. Acad. Sci. USA* **88**:9360–9364. (1991).
26. Cathcart, R., E. Schwiers, and B. N. Ames. Detection of picomole levels of hydroperoxides using a fluorescent dichlorofluorescein assay. *Anal. Biochem.* **134**:111–116 (1983).
27. Uchiyama, M., and M. Mihara. Determination of malondialdehyde precursor in tissues by thiobarbituric acid. *Anal. Biochem.* **86**:271–298 (1978).
28. Hedley, D., and S. Chow. Fluorocytometric measurement of lipid peroxidation in vital cells using parinaric acid. *Cytometry* **13**:686–692 (1992).
29. Stigall, D. L., Y. M. Galante, and Y. Hatefi. Preparation and properties of complex V. *Methods Enzymol.* **55**:308–315 (1979).
30. Schreiber, E., P. Matthias, M. M. Mueller, and W. Schaffner. Eukaryotic expression vector for the analyses of mutant proteins. *Nucleic Acid Res.* **17**:6418–6419 (1989).
31. Fried, M., and D. M. Crothers. Equilibria and kinetics of Lac repressor operator interactions by polyacrylamide gel electrophoresis. *Nucleic Acid Res.* **9**:6505–6512 (1981).
32. Kukielka, E., E. Dicker, and A. I. Cederbaum. Increased production of reactive oxygen species by rat liver mitochondria after chronic ethanol treatment. *Arch. Biochem. Biophys.* **309**:377–386 (1994).
33. Sen, R., and D. Baltimore. Inducibility of k immunoglobulin enhancer-binding protein NF-kB by a posttranslational mechanism. *Cell* **47**:921–928 (1986).
34. García-Ruiz, C., A. Morales, A. Colell, A. Ballesta, J. Rodés, N. Kaplowitz, and J. C. Fernández-Checa. Feeding S-adenosyl-L-methionine attenuates both ethanol-induced depletion of mitochondrial glutathione and mitochondrial dysfunction in periportal and perivenous rat hepatocytes. *Hepatology* **21**:134–141 (1995).
35. Martensson, J., and A. Meister. Mitochondrial damage in muscle occurs after marked depletion of GSH and is prevented by giving GSH-ester. *Proc. Natl. Acad. Sci. USA* **86**:471–475 (1989).
36. Martensson, J., A. Jain, W. Frayer, and A. Meister. Glutathione metabolism in the lung: inhibition of its synthesis leads to lamelar body and mitochondrial defects. *Proc. Natl. Acad. Sci. USA* **86**:5296–5300 (1989).
37. Meredith, M., and D. J. Reed. Depletion *in vitro* of mitochondrial GSH in rat hepatocytes and enhancement of lipid peroxidation by adriamycin and BCNU. *Biochem. Pharmacol.* **32**:1383–1388 (1988).
38. Castilho, R., F. A. J. Kowaltowski, A. R. Meinicke, E. J. H. Bechara, and A. E. Vercesi. Permeabilization of the inner mitochondrial membrane by calcium ions is stimulated by t-butyl hydroperoxide and mediated by oxygen species generated by mitochondria. *Free Rad. Biol. Med.* **18**:479–486 (1995).
39. Castilho, R., F. A. J. Kowaltowski, A. R. Meinicke, and A. E. Vercesi. Oxidative damage of mitochondria induced by Fe(II) citrate or t-butyl hydroperoxide in the presence of calcium: effect of coenzyme Q redox state. *Free Rad. Biol. Med.* **18**:55–59 (1995).
40. Schulze-Osthoff, K., R. Beyaert, V. Vandevoorde, G. Haegeman, and W. Fiers. Depletion of the mitochondrial electron transport abrogates the cytotoxic and gene-inductive effect of TNF. *EMBO J.* **12**:3095–3104 (1993).
41. Abate, C., L. Patel, F. J. Rauscher III, and T. Curran. Redox regulation of Fos and Jun DNA binding activity *in vitro*. *Science (Washington D. C.)* **249**:1157–1161 (1990).
42. Schreck, R., B. Meier, D. Männel, W. Dröge, and P. Bauerle. Dithiocarbamates as potent inhibitors of NF-kB activation in intact cells. *J. Exp. Med.* **175**:1181–1194 (1992).
43. Schulze-Osthoff, K., A. C. Bakker, B. Vanhaesebroeck, R. Beyaert, W. A. Jacob, and W. Fiers. Cytotoxic activity of tumor necrosis factor is mediated by early damage to mitochondrial functions. *J. Biol. Chem.* **267**:5317–5323 (1992).
44. Fernández-Checa, J. C., M. Ookhtens, and N. Kaplowitz. Effects of chronic ethanol feeding on rat hepatocytic glutathione: relationship of cytosolic glutathione to efflux and mitochondrial sequestration. *J. Clin. Invest.* **83**:1247–1252 (1989).
45. Newmeyer, D. D., D. M. Farschon, and J. C. Reed. Cell-free apoptosis in Xenopus egg extracts: inhibition by Bcl-2 and requirement for an organelle fraction enriched in mitochondria. *Cell* **79**:353–364 (1994).
46. Fujii, Y., M. E. Johnson, and G. J. Gores. Mitochondrial dysfunction during anoxia/reperfusion injury of liver sinusoidal endothelial cells. *Hepatology* **20**:177–185 (1994).

Send reprint requests to: José C. Fernández-Checa, Ph.D., Liver Unit, Hospital Clinic i Provincial, Villarroel, 170, Barcelona 08036, Spain.